Proc. Natl. Acad. Sci. USA
Vol. 83, pp. 2879–2883, May 1986
Biophysics

Contact pressures in the human hip joint measured *in vivo*

(synovial joints/osteoarthritis/postsurgical rehabilitation/joint replacement prostheses/gait analysis)

W. A. HODGE*, R. S. FIJAN†, K. L. CARLSON†, R. G. BURGESS†, W. H. HARRIS*, AND R. W. MANN†‡

*Department of Orthopaedic Surgery, Massachusetts General Hospital, Boston, MA 02114; and †Department of Mechanical Engineering, Massachusetts Institute of Technology, Cambridge, MA 02139

Contributed by R. W. Mann, December 26, 1985

ABSTRACT **The pressures on human articular cartilage have been measured *in vivo*. An instrumented femoral head prosthesis that telemeters interarticular pressure at 10 discrete locations 253 times per second was implanted in apposition to natural acetabular cartilage. Data were acquired during surgery, recovery, rehabilitation, and normal activity, for longer than 1 year after surgery. Pressure magnitudes were synchronized with body-segment kinematic data and foot–floor force measurements so as to locate transduced pressure areas on the natural acetabulum and correlate movement kinematics and dynamics with local cartilage pressures. The data reveal very high local (up to 18 MPa) and nonuniform pressures, with abrupt spatial and temporal gradients, that correlate well both in magnitude and distribution with *in vitro* data and computer simulations of synovial joint mechanics. Peak pressures *in vivo* are, however, considerably higher than pressures measured *in vitro* under the putative forces experienced by the joint in life, particularly in normal movements where cocontraction occurs in agonist and antagonist muscles across the hip joint. Thus, extant gait-analysis studies which apply inverse Newtonian calculations to infer joint forces establish the lower limit on such forces, since such analyses include only the net muscular torques about the joint and cannot account for the contribution of the increment in joint force due to muscular cocontraction. Our data also contribute to the understanding of normal synovial joint tribology and the possible role of mechanical factors in the deterioration evident in osteoarthritis. Further, design criteria for both partial and total hip replacement prostheses and specific aspects of rehabilitation protocols following hip surgery (e.g., the extent to which crutches and canes unload the hip joint) warrant reconsideration in light of the extraordinary high pressures measured during the activities of daily living.**

The maximum resultant force across the human hip joint during walking and running had been first estimated (1–3) and then measured *in vivo* (4–6) at from 2.5 to 5.8 times body weight, but the local pressures and pressure distribution between opposing cartilage layers in life have not been reported. Such knowledge is essential to understanding the physiology and pathology of human articular cartilage. How the opposing thin (1–3 mm) layers of articular cartilage in synovial joints distribute high loads across mating joint areas is essential to understanding the remarkable tribology (7) of normal joints—high load carriage, low coefficients of friction (0.01–0.002), and long life—and may illuminate the role of mechanical factors in the etiology of osteoarthritis. Current opinion on the pathogenesis of this widely prevalent [estimated to afflict more than forty-million persons in the United States in 1962–64 (8)] and frequently incapacitating chronic disease (9) implicates focal mechanical stress on or in cartilage (10). We report here the direct measurement of cartilage surface pressures in the human hip joint *in vivo*.

Prior human joint pressure data have all resulted from loading cadaverous tissue. Average pressures over large areas of cartilage have been calculated by using dye transfer to estimate contact area (11) or have involved excising concentric rings of acetabular cartilage which were then loaded to measure cartilage compression, which data were used to estimate joint pressure (12). Such techniques estimated average pressures in the range of 2.0–3.0 MPa at 3 times body-weight load and assume that global pressure distributions are gradual and well-behaved, ranging from uniform to sinusoidal axisymmetric about the load vector. More recently, direct focal measurements have employed small pressure transducers mounted in an endoprosthesis replacing the natural femoral head (13, 14), located in subchondral bone just below the intact cartilage (15), or sandwiched into recesses cut into the articular cartilage surface (16). In general agreement with each other, these more detailed studies, when compared with the earlier experiments, give about the same average pressures but otherwise produce a quite different topology of cartilage pressure distribution. Variations in local pressures can be quite abrupt spatially, the isobar contours are very irregular and idiosyncratic, and high local pressures are measured. For example, at 2.6 body-weight force at the hip (appropriate for the single-leg support phase of level walking), the peak local cartilage stress is 6.78 MPa, with a mean pressure of 2.14 MPa (13, 14). Computer simulations of the global hip joint in level walking, employing mathematical models based on ultrasonically acquired data on cartilage layer geometries (17) and constitutive properties (18), have produced comparable results (19).

Experimental Procedure. The *in vivo* data reported here were produced by the same pressure-instrumented endoprosthesis technique used previously to produce *in vitro* data (13, 14). Recesses (3.96 mm diameter) were electron-discharge-machined from inside the cobalt/chromium/carbon-alloy, pseudofemoral head shell at 14 locations, leaving 0.445 mm thick, slightly convex diaphragms whose external surfaces are integral with the polished sphere of the endoprosthesis. Diaphragm deflection due to pressure from the opposing acetabular articular cartilage is center-point detected and measured with a four-arm strain-gauge bridge diffused onto a single-silicon-crystal cantilever beam. In the *in vitro* studies (13, 14), the electrical signals were hard-wired to the computer analog/digital input. For the *in vivo* instrument (20), the pressure transducers are serially excited by an oscillator and a multiplexer switch, with each isolated transducer output modulating an FM telemetry transmitter, all contained within the hermetically sealed endoprosthesis ball. The resulting pulse-amplitude-modulated signal, together

The publication costs of this article were defrayed in part by page charge payment. This article must therefore be hereby marked "*advertisement*" in accordance with 18 U.S.C. §1734 solely to indicate this fact.

‡To whom reprint requests should be addressed at: Massachusetts Institute of Technology, Room 3-144, 77 Massachusetts Avenue, Cambridge, MA 02139.

with high and low calibration pulses, is transmitted at a frame-repetition rate of 253 Hz from an antenna at the distal end of the prosthesis intermedullary stem. The passive electronics are powered inductively from an externally mounted 100-kHz transmitting loop. By avoiding internal batteries, biocompatibility is enhanced, and the prosthesis instrumentation can function for the entire implantation life. Fig. 1 illustrates the prosthesis prior to electron-beam welding of the femoral head equator, sterilization of the internal components with ethylene oxide, hermetic sealing, and final polishing.

Equipment to receive, record, and process data during surgery, recovery, rehabilitation, and normal activities is comprised of a 100-kHz power supply with two radiofrequency coupling coils, one fitting directly over the prosthesis antenna, for powering the electronics before and during implantation, and a second, thigh-encircling coil used immediately after implantation and subsequently in recovery, in rehabilitation, and in the activities of daily living; an external FM antenna and receiver; a synchronizer and demultiplexer; a normalizer for individual transducer recalibration; a portable digital computer for real-time data processing and data storage (PDP 11/03, Digital Equipment, Maynard, MA); a loading tool with integral force-measuring transducer which accepts the instrumented prosthesis and small rf power coupling coil; and a visual display with light-emitting diodes (LEDs) corresponding to pressure-transducer location on the femoral head surface, with LED intensity proportional to pressure level, together with a numerical display of pressure magnitude.

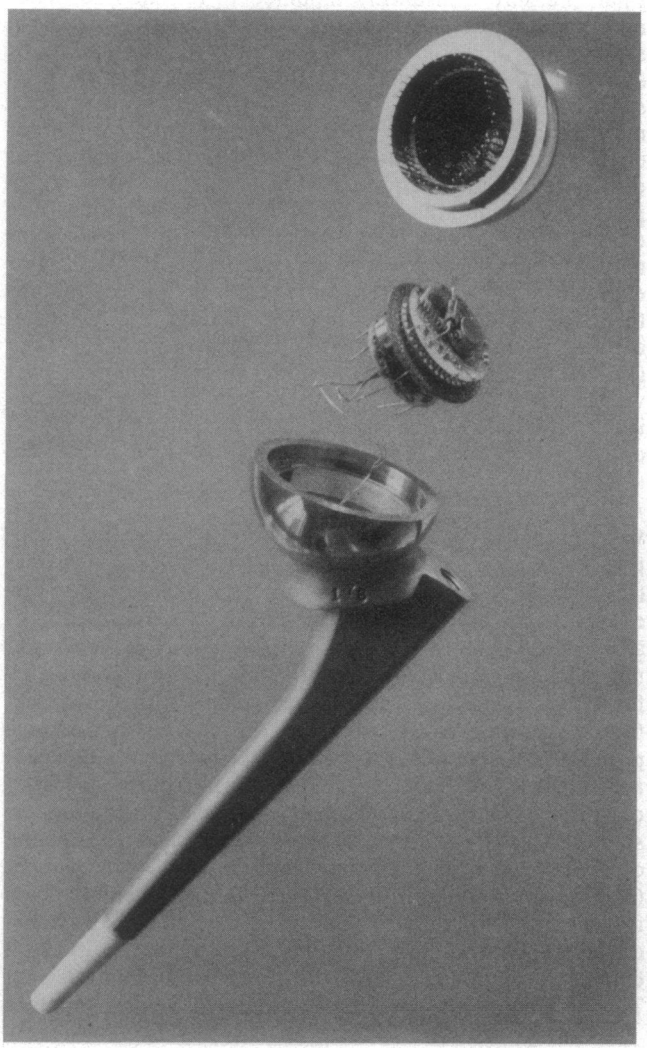

FIG. 1. Instrumented prosthesis showing pressure-instrumented pseudofemoral head hemisphere, electronics package, and antenna on distal end of intermedullary stem.

Extensive testing and calibration over the range of possible pressures and temperatures anticipated *in vivo* were conducted in temperature-controlled hydrostatic pressure vessels, in a hip simulator that reproduces the kinematics and dynamics of gait (21) and in cadaver insertions using the operating room data-acquisition and -recording equipment. In the prosthesis implanted, the calibration data for 4 of the 14 pressure transducers were not consistent with rigorous specifications; although data from all transducers were always recorded, only that from the 10 satisfactory transducers is reported.

In June 1984, an active 73-year-old woman (68 kg, 1.68 m) with a displaced fracture of the right femoral neck consented to the implantation of the instrumented endoprosthesis in substitution for the standard orthopaedic device, as illustrated in the frontal plane x-ray of Fig. 2. The exposed acetabular cartilage was carefully inspected visually to ensure that it was normal. The importance of proper fit of any endoprosthesis to achieve optimal distribution of interarticular pressure has been demonstrated by prior studies (14, 22). Accordingly, to ascertain the fit between the 47.5-mm-diameter spherical prosthesis head and the concavity of the natural acetabulum, three techniques were employed. First, the excised natural femoral head was sized at 47.5 mm using "go, no-go" gauges; next, clear acrylic hemispheres in 1-mm-diameter increments were observed as they contacted the acetabular surface, with best fit noted between 47 and 48 mm; finally, the instrumented prosthesis was loaded against the acetabulum and the individual pressure transducer readings were checked, using the LED display to visualize the distribution of load bearing.

Interpretation of the pressure data requires concurrent acquisition of data on the kinematics and dynamics of the subject's movement. Through correlation of these simultaneous data streams, the locations of the femoral head transducers on the acetabular cartilage surface are calculated using kinematic data on the position and orientation of the subject's thigh segment relative to her pelvis. Similar kinematic data, but also including that from the shank and foot, permit computer graphics displays of the subject's pelvis/thigh/shank/foot positions and orientations simultaneous

FIG. 2. Frontal plane x-ray of pelvis–thigh region, showing instrumented prosthesis.

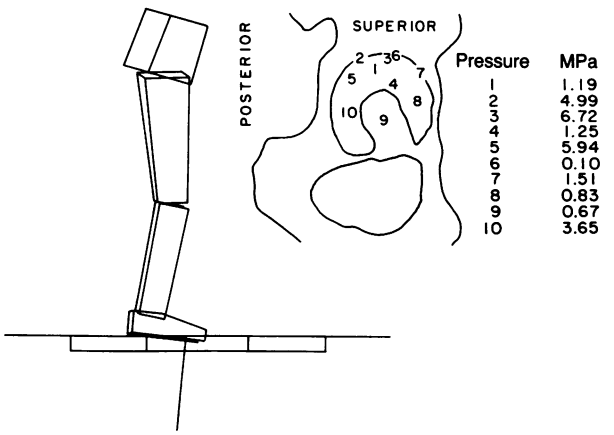

FIG. 3. Pressures, 6 months after surgery, at 10 locations on acetabular cartilage as the patient passes through the single-leg stance of normal walking, together with the kinematics of the limb segments and pelvis of the instrumented leg, and the foot–floor force vector, representing 103% of body weight.

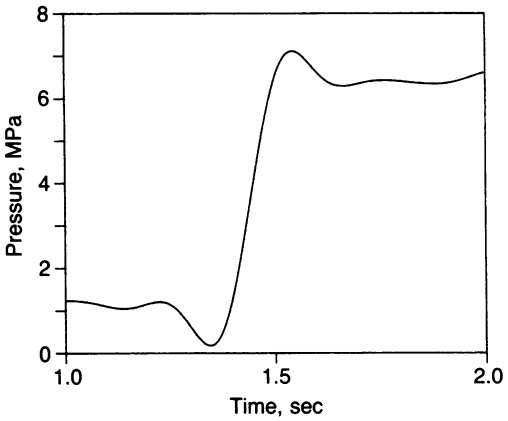

FIG. 4. Example of a rapid pressure increase during stair-climbing 6 months after surgery.

with display of the transducer locations and the corresponding pressures (Fig. 3).

The kinematic data are acquired via a hardware/software system (23, 24) employing two optoelectronic Selspot II cameras (Selective Electronics, Partille, Sweden) and an extensive computer program with the acronym TRACK (Massachusetts Institute of Technology, Cambridge, MA), operating on two minicomputers (PDP 11/60, Digital Equipment) linked with DECnet. Photostereogrammetric reconstruction of serially illuminated infrared LEDs and the aggregation of individual LED three-dimensional position data from multiple LEDs on rigid arrays mounted on the body segments permit precise calculation of body-segment 6 degrees of freedom, positions within 1 mm in a 2-m^3 viewing volume, and orientations within 20 milliradians. The integration into the pressure and kinematic data stream of the concurrent foot–floor force vector data from two multicomponent force-measuring platforms (Type 9281A, Kistler Instrumente, Wintorthur, Switzerland) permits comparison of internal pressures with external forces. Kinematic and force–platform data are acquired at 153 or 200 Hz, which assures high-fidelity recording of the frequency components of gait (25). In the data reported here, high-frequency cut-off filters have been applied to the raw data, the cut-off frequencies being 10 Hz for the pressure data and 15 Hz for the kinematic data.

Data were collected during surgery, recovery, rehabilitation, and normal activities—initially several times a day; then at several-month intervals. The abundant data will be reported in detail in articles focused on surgical, rehabilitation, biomechanical, and synovial joint aspects of the research; here we present representative data of scientific interest.

RESULTS AND DISCUSSION

Fig. 3 correlates body-segment kinematics and the foot–floor force vector during the stance phase of level walking with the positions of the transducers on the acetabulum and the pressure magnitudes. The nonuniform pressures and high spatial gradients are quite consistent with similar data acquired *in vitro* (13, 14, 16). Thus earlier conclusions, based on *in vitro* study by others, that the pressure distribution in the human hip is essentially uniform at high load (11) or sinusoidal (12) are incorrect, as are their estimates of much lower local pressure magnitudes.

The temporal character of the pressure data, arising as it does from normal human activities imposing movement and forces on a major synovial joint, is of interest in understanding the tribology of these remarkable bearings. Current research by others on cartilage mechanics almost invariably involves tests on small plugs of cartilage and bone under quasistatic loading conditions (26). The plugs are either restrained or allowed to expand radially; the loading surface is usually permeable, allowing unrestricted fluid-flow axially as the fluid-saturated cartilage is compressed; and tare loads are always applied before data are recorded.

Unfortunately, these boundary conditions do not replicate the reality of normal cartilage in the global joint *in situ* (18), where radial outflow from the compressed cartilage must pass through the interarticular space, which is severely restricted by the tortuosity of the extremely narrow clearance space between the two closely congruent mating surfaces (27). The tests reported here describe the temporal performance of the global joint under natural loading conditions. Fig. 4 gives pressure vs. time for one transducer during stair-climbing, showing an increase of 7 MPa in 0.15 sec. These *in vivo* measurements demonstrate the effectiveness of the seal between the acetabular cartilage and the pseudofemoral sphere in maintaining a high-pressure, fluid film as fluid in the saturated cartilage layer is exuded as the cartilage is loaded and compressed. This self-pressurized fluid film then supports well over 90% of the load, with the small remainder carried by the solid stress on the cartilage matrix, thereby maintaining the integrity and effectiveness of the interarticular seal. Major load support by the fluid film also accounts for the low frictional coefficients reported for mammalian synovial bearings (28). The *in vivo* measurements and interpretation are consistent with the "weeping lubrication" theory of McCutchen (29) and the predictions of our computer simulations of the global joint (19)[§]. The highest pressure rate recorded to date is 107 MPa/sec, occurring in the lower posterior region of the acetabulum as the subject rose from a 45-cm chair.

Concurrent comparison of the temporal aspects of pressure data and of the external force vector enhances our quantitative understanding of the role of the musculature in human movement. Fig. 5 compares a record of the vertical foot–floor force with the pressure magnitude at a single pressure transducer during normal level walking. Reasonable time correlation between the two signals is shown, but note that pressure rise precedes the application of external foot–floor force. The musculature across the hip contracts to anticipate the coming heel strike, thereby increasing the impedance of

[§]Tepic, S., Macirowski, T. & Mann, R. W., Fourth Meeting of the European Society of Biomechanics, September 24–26, 1984, Davos-Platz, Switzerland.

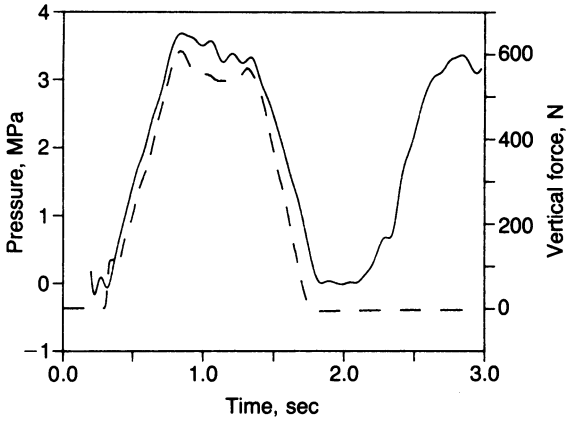

FIG. 5. Comparison of pressure from transducer in load-bearing region of acetabulum (solid line) and vertical force between foot and floor (broken line) during normal level walking, 6 months after surgery.

the joint [a topic of current interest in biomechanics, neuroscience, and robotics (30)]. Prior energy consumption evaluations and muscle electromyographic studies of gait have shown that the degree of muscle contraction in normal level walking is modest compared to the capacity of the muscles (31). In a more energetic task (Fig. 6), the subject stands on the force plates, rises on her toes (thereby massively cocontracting the musculature of the lower extremity to stabilize her body mass within the smaller support area), and then relaxes so as to fall forcefully onto her heels. Hip muscle forces are apparent in the high-pressure trace while in the elevated position. As she relaxes from the extreme plantar-flexed position, the hip pressure falls prior to any external force registration on the force plate. The force-plate record shows an impulse >1.5 times body weight at heel strike, but the hip pressure continues to fall, with only slight evidence of the heel strike being transmitted through the leg to the hip joint. The force-attenuation capacity of the skeleton, joints, muscle, and other soft tissue is clear. Fig. 7 also illustrates the muscular contribution to force across a joint. At mid-rise from a chair, hip musculature cocontraction is stabilizing the joint, in addition to providing a net torque. At the time shown, the foot–floor force is supporting 45% of body weight, but the maximal pressure reading is 7.14 MPa. Compare this with Fig. 3 for the stance phase of gait where,

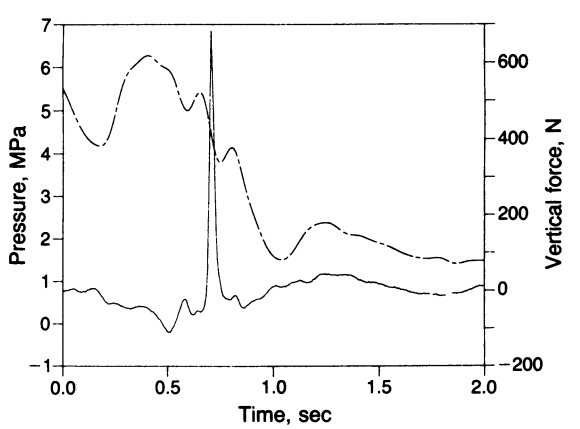

FIG. 6. Comparison of pressure from transducer in load-bearing region of acetabulum (filtered at 8 Hz, broken line) and vertical force between foot and floor (solid line) as the subject plantar-flexes on both toes and then drops abruptly onto both heels, 6 months after surgery.

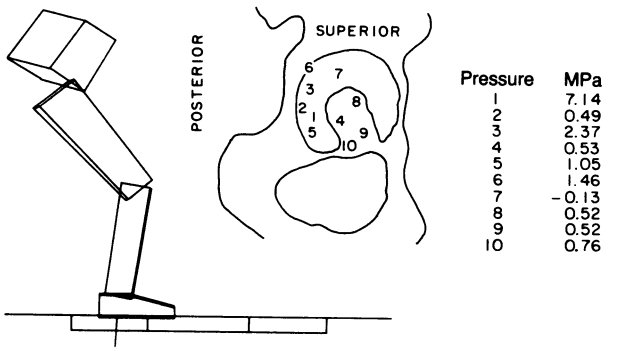

FIG. 7. Pressures, 6 months after surgery, at 10 locations on acetabular cartilage as the patient passes through mid-rise during sitting to standing, together with the kinematics of the limb segments and pelvis of the instrumented leg, and the foot–floor force vector, representing 45% of body weight.

for a force vector of 103% of body weight, the highest pressure is but 6.72 MPa, and, of course, located in a different region of the acetabulum.

An important consequence of these *in vivo* indications of the role of muscle cocontraction in normal activities applies to analyses where kinematic and foot–floor data are incorporated into an inverse Newtonian formulation to estimate the forces occurring across the joints internally. Since such study can evaluate only the net forces that caused the observed motion, and cocontraction is shown by our data to be present even in level walking, dynamic estimates of gait analysis must be understood to constitute the lower bound on the range of forces the joints are experiencing.

Among other applications, dynamic estimations from gait studies, usually data from level walking, are used to define load specifications in the design of joint replacement prosthesis. Since our data show that normal daily activities, such as stair-climbing and rising from a chair, cause much higher pressures (due to muscle cocontraction) and therefore impose higher forces on the joint, such design specifications warrant reconsideration.

The data also suggest that the time, subsequent to surgical intervention, involved in the recuperation of muscles depends on the activity. Fig. 8 compares pressure at one transducer vs. time during sitting to standing at 6 months and at 1 year after surgery, when the maximum pressure reaches 18 MPa. More recent data at 15 months show even higher pressures, indicating that she continues to contract her musculature ever more energetically in this maneuver. Data

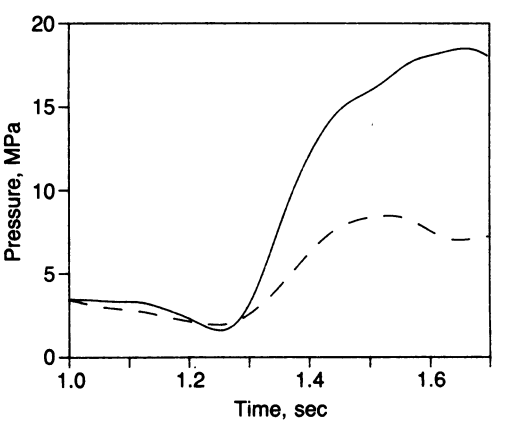

FIG. 8. Pressure vs. time for sitting to standing, 6 months (broken line) and 1 year (solid line) after surgery.

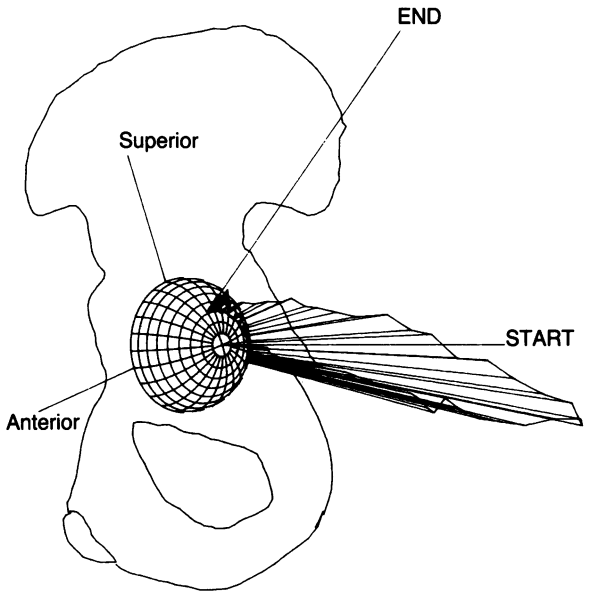

FIG. 9. Pressure magnitude and position on the acetabulum as the subject rises from a chair, 11 months after surgery.

comparisons for level walking, however, indicate no further rises in pressure after 1 year postoperatively.

Beyond illuminating the issues discussed above, this rich and continuing data source from a most cooperative subject fitted with a closely congruent, instrumented prosthesis is contributing to long-term survival information on endoprosthetic hemiarthroplasties (32). The data are also challenging many traditional patient management and rehabilitation protocols applied subsequent to major hip surgery of all kinds. For example, since corresponding local acetabular pressures are only 5% greater with a cane than with a crutch, patients might be advanced to cane-usage more rapidly than is the current practice.[¶] Beyond continued data acquisition from this one subject and the planning of future implantations, current efforts include development of techniques for compressing the copious data stream and enhancing its interpretation, such as the computer graphics display of Fig. 9.

[¶]Hodge, W. A., Fijan, R. S., Carlson, K. L., Riley, P. O., Mann, R. W. & Harris, W. H., Thirty-Second Annual Orthopaedic Research Society Meeting, January 21–24, 1985, New Orleans, LA.

Design of the instrumented prosthesis was supported by grants from the National Science Foundation, the National Institute for General Medical Sciences, the Medical Foundation, Inc., of Massachusetts, the Easter Seal Research Foundation, and the Germeshausen Professorship at the Massachusetts Institute of Technology. Development was supported in part by the Smith Petersen Fund at the Massachusetts General Hospital and by National Institutes of Health Grant AM16116. Fabrication and implantation were supported by the Whitaker Professorship, the Newman Laboratory Fund, and the Sloan Fund for Basic Research, all at the Massachusetts Institute of Technology; the William H. Harris Foundation at the Massachusetts General Hospital; the Arthritis Foundation of Massachusetts; and the June Rockwell Levy Foundation. Data acquisition, processing, and interpretation were supported in part by Grant G00830074 from the National Institute of Handicapped Research, Department of Education.

1. Inman, V. T. (1947) *J. Bone Surg. Am.* **29**, 606–619.
2. Denham, R. A. (1959) *J. Bone Jt. Surg. Br.* **41(B)**, 550–557.
3. Paul, J. P. (1965) in *Biomechanics and Related Bio-Engineering Topics*, ed. Kenedi, R. M. (Pergamon, London), pp. 369–380.
4. Rydell, N. W. (1966) *Acta. Orthop. Scand. Suppl.* **88**, 9.
5. English, T. A. & Klivington, M. (1979) *J. Biomed. Eng.* **1**, 111–115.
6. Brown, R. H. (1985) *Trans. Orthop. Res. Soc.* **10**, 283 (abstr.).
7. Freeman, M. A. R. (1979) in *Adult Articular Cartilage*, ed. Freeman, M. A. R. (Pitman Med., Kent, England), 2nd Ed., pp. 291–460.
8. Gordon, T. (1968) in *Population Studies of the Rheumatic Diseases*, ed. Wood, P. H. (Excerpta Med., New York), p. 391.
9. Kelsey, J. L., Pastides, H. & Bisbee, G. E., Jr. (1978) *Musculoskeletal Disorders: Their Frequency of Occurrence and Their Impact on the Population of the United States* (Prodist, New York).
10. Lee, P., Rooney, P. J., Sturrock, R. D., Kennedy, A. C. & Dick, W. C. (1974) *Arthritis Rheum.* **3**, 189–218.
11. Greenwald, A. S. & O'Connor, J. J. (1971) *J. Biomech.* **4**, 507–528.
12. Day, W. H., Swanson, S. A. V. & Freeman, M. A. R. (1975) *J. Bone Jt. Surg. Br.* **57**, 302–313.
13. Rushfeldt, P. D., Mann, R. W. & Harris, W. H. (1979) *Science* **204**, 413–415.
14. Rushfeldt, P. D., Mann, R. W. & Harris, W. H. (1981) *J. Biomech.* **14**, 315–323.
15. Mizrahi, J., Solomon, L. & Kaufman, B. (1980) *Phys. Med. Biol.* **25**, 1181 (abstr.).
16. Brown, T. D. & Shaw, D. T. (1982) *J. Biomech.* **15**, 329–333.
17. Rushfeldt, P. D., Mann, R. W. & Harris, W. H. (1981) *J. Biomech.* **14**, 253–260.
18. Tepic, S., Macirowski, T. & Mann, R. W. (1983) *Proc. Natl. Acad. Sci. USA* **80**, 3331–3333.
19. Tepic, S., Macirowski, T. & Mann, R. W. (1984) *Proc. Summer Comp. Simul. Conf.* (Soc. Comp. Simul., La Jolla, CA), Vol. 2, pp. 834–839.
20. Carlson, C. E., Mann, R. W. & Harris, W. H. (1974) *IEEE Trans. Biomed. Eng.* **BME-21**, 257–264.
21. Mann, R. W., Rushfeldt, P. D., Palmer, D. W., Tepic, S. & Macirowski, T. (1983) in *1983 American Society of Mechanical Engineers Advances in Bioengineering*, ed. Bartel, D. (Am. Soc. Mech. Eng., New York), pp. 108–319.
22. Harris, W. H., Rushfeldt, P. D., Carlson, C. E., Scholer, J. M. & Mann, R. W. (1975) in *The Hip: Proceedings of the Third Open Scientific Meeting* (Mosby, St. Louis, MO), pp. 93–98.
23. Mann, R. W. & Antonsson, E. K. (1983) *Bull. Hosp. Jt. Dis.* **43**, 137–146.
24. Mann, R. W., Rowell, D., Dalrymple, G., Conati, F., Tetewsky, A. T., Ottenheimer, D. & Antonsson, E. (1983) in *Biomechanics VIII-B* (Human Kinetics, Champaign, IL), pp. 1104–1112.
25. Antonsson, E. K. & Mann, R. W. (1985) *J. Biomech.* **18**, 39–47.
26. Holmes, M. H., Lai, W. M. & Mow, V. C. (1985) *J. Biomech. Eng. Trans. Am. Soc. Mech. Eng.* **107**, 206–218.
27. Kenyon, D. E. (1980) *J. Biomech.* **13**, 129–134.
28. Linn, F. C. (1969) *J. Lubr. Technol.* **91**, 329–341.
29. McCutchen, C. W. (1962) *Wear* **5**, 1–17.
30. Hogan, N. (1985) *J. Dyn. Syst. Meas. Control Trans. Am. Soc. Mech. Eng.* **107**, 1–24.
31. Patriarco, A. G., Mann, R. W., Simon, S. R. & Mansour, J. M. (1981) *J. Biomech.* **14**, 513–525.
32. Sreide, O., Skjaerven, R. & Alho, A. (1982) *Acta Orthop. Scand.* **53**, 79–94.